ELECTROCHEMICAL DISSOLUTION OF IRON(III) HYDROXY-OXIDES: MORE INFORMATION ABOUT THE PARTICLES

Tomas GRYGAR

Institute of Inorganic Chemistry,
Academy of Sciences of the Czech Republic, 250 68 Rez near Prague, Czech Republic

Received February 21, 1995
Accepted August 29, 1995

The process of reductive dissolution of α-Fe_2O_3, Ba-hexaferrite, α-FeOOH, γ-Fe_2O_3, γ-FeOOH, and ferrihydrite can be monitored continuously by abrasive stripping voltammetry and chronoamperometry to obtain information about homogeneity of reactivity and about the particle size of the pure phases and mixtures. Phase parameters (rate constant and charge transfer coefficient) and the geometrical factor γ, which is independent on the specific surface area, can be assigned to a phase-pure sample in the given medium. Differences in reactivity of the hydroxy-oxides are documented, and the dependence of reactivity of the α-Fe_2O_3 samples on the preparation procedure is characterized. The electrochemical techniques can also be employed to investigate changes in the particles during phase transformations.
Key words: Abrasive stripping voltammetry; Oxides Fe(III).

The dissolution of iron(III) hydroxy-oxides in acid medium can be described by Eqs (*A*) and (*B*), in which the symbols (s) and (aq) denote the solid phase and the solution, respectively.

$$1/2\ Fe_2O_3(s) + 3\ H^+ + n\ e \longrightarrow (1 - n)\ Fe^{3+}(aq) + n\ Fe^{2+}(aq) + 3/2\ H_2O \qquad (A)$$

$$FeOOH(s) + 3\ H^+ + n\ e \longrightarrow (1 - n)\ Fe^{3+}(aq) + n\ Fe^{2+}(aq) + 2\ H_2O \qquad (B)$$

The reactions are phase selective and their course is affected by the pH and by the presence of other chemisorbing ions. The dissolution can be conducted as a proton-promoted process at $n = 0$ (refs[1–5]) or as a reductive process at $n > 1$ (reduction with sulfane[4,5], ascorbic acid[6], or electrochemical[7]). Reactions (*A*) and (*B*) are employed in syntheses (elimination of amorphous impurities from goethite[8]), for the speciation of Fe in sediments[6], and indirectly also for the speciation of heavy metals bonded to low-crystalline oxidic compounds of Fe and Mn in sediments and soils[9]. Synthetic iron hydroxy-oxides can be evaluated with respect to their specific properties such as anisotropy of goethite dissolution[1,2,10] and the course of dissolution of various hematite particles[11]. The chemical dissolution experiment, however, is rather time consuming; convenient is the application of the electrochemical dissolution method based on the

use of an active paste[12], or the abrasive stripping voltammetry technique[13,14] (henceforth AbrSV), which both enable the reaction to be monitored continuously by measuring electrical quantities of the system, offering the opportunity to vary the reaction rate over a wide region by choosing a suitable potential[10]. The application of the active paste method, however, is associated with the creation of a large quantity of Fe^{n+} ions within a limited volume of the binder, which affects the measurement[15]. Therefore, the AbrSV method seems to be better suited to the examination of the whole irreversible reaction.

The course of the reductive dissolution of ferrihydrite[8] in excess ascorbic acid at pH 3 has been described[6] by a kinetic equation, viz.

$$\frac{J}{N_0} = k\left(\frac{N}{N_0}\right)^{\gamma}, \qquad (1)$$

where $J = \mathrm{d}N/\mathrm{d}t$ is the mass flow of the forming Fe^{2+} ions. The reaction course is characterized by the pseudo-first order rate constant k and parameter γ, whose magnitude is 2/3 for monodisperse isotropic spherical particles, approaches 1 for single-phase particle sets possessing a homogeneous size distribution[6,16], and is much larger than 1 in particle sets with a broad rate constant distribution[6].

If the proton-promoted dissolution rate in a non-complexing medium is much smaller than during the reduction of Fe(III), and the value of n in Eqs (*A*) and (*B*) is 1 (all dissolved iron is in the form of Fe^{2+}, ref.[7]), then Eq. (*1*) can be transformed into Eq. (*2*) by using Faraday's law:

$$\frac{I}{Q_0} = k\left(\frac{Q}{Q_0}\right)^{\gamma} \qquad (2)$$

and the course of dissolution can be monitored chronoamperometrically or voltammetrically[10,17]. The rate constant k in Eq. (*3*) obeys the basic electrochemical equation (*3*):

$$k = k_0 \exp\left(-\frac{\alpha n F}{RT} E\right), \qquad (3)$$

where k_0 is the rate constant at the potential of the reference electrode. The validity of this equation, however, is limited by the requirement of an infinite mass transport rate (i.e. by the constraint that the reaction rate must not approach that for the diffusion-controlled dissolution[17]). Provided that Eq. (*3*) applies, parameter γ in Eq. (*2*) carries the same information as in Eq. (*1*), which holds similarly as if protons as well as the reducing substance are present in excess at the reacting surface in the course of common suspension dissolution[6].

The following equation has been derived to describe the position of the DC voltammetric peak during the reaction of solid monodisperse particles in a paste electrode[12]:

$$E_p = E_0 - \frac{RT}{\alpha nF} \ln\left(\frac{\alpha nF}{RT}\nu\right) + \frac{RT}{\alpha nF} \ln k \quad . \qquad (4)$$

The present work was aimed at ascertaining whether Eq. (*4*) is applicable to the electrochemical dissolution of oxidic compounds of trivalent iron and whether parameter γ is well suited to the characterization of synthetic samples with respect to their particle homogeneity and phase composition.

EXPERIMENTAL

Electrochemical Measurements

The measurements were performed on a PA4 polarograph interfaced to XY4106 and XY4260 plotters (Laboratorni pristroje, Prague). Voltammograms were measured applying the differential pulse mode using pulses of –50 mV in 1 s periods unless stated otherwise. The working electrode was prepared by evacuation of a spectral graphite rod (Elektrokarbon Topolcany, Slovakia) in molten paraffin (m.p. 54–55 °C). All potentials reported in this paper are relative to the saturated calomel electrode (SCE). A Pt sheet was used as the counter-electrode.

Sample was applied to the electrode by the conventional AbrSV procedure[13], i.e. by rubbing a few milligrams of sample on a filter paper and wiping the freely sticking particles with cotton wool[10,17]. The typical amount of sample so deposited corresponded to 1 to 20 mC (1–20 μg). The measuring surface of the electrode was then immersed slightly below the supporting electrolyte level[13,14]. The counter-electrode was separated by a diaphragm from the working and reference electrodes. The electrode surface was restored by polishing with a paste based on silicone oil and Cr and Si oxides.

The following supporting electrolytes were used: 0.1 M HCl, 0.2 M chloroacetate buffer with KCl at a concentration of 0.1 mol l^{-1} (pH 2.7; henceforth MCAB), 0.2 M solution of monochloroacetic acid with KCl at a concentration of 0.1 ml l^{-1} (pH 1.8; henceforth MCAA), and 0.1 M solution of potassium hydrogen oxalate (pH 2.5; henceforth KHOx).

Iron Compounds

Hematite (α-Fe_2O_3). Hydrothermal hematite with approximately 3% crystal water[18,19] (hematite 1); sample obtained from hematite 1 by dehydration at 500 °C for 1 h – specific surface and particle shape as with the starting sample (hematite 2); sample obtained by heating ferrihydrite 2 at 300–500 °C (hematite 3); commercial pigment Bayer No. 130 (Bayer, Germany) (hematite 4); products of hydrothermal transformation of ferrihydrite[8] at 90, 110, and 170 °C (hematite 5); product of transformation of goethite by mechanical grinding[20] (hematite 6).

Maghemite (γ-Fe_2O_3). Commercial SCP 21 recording material (Société Chimique de Provence, France) (maghemite 1); magnetite sample heated in air at 250 °C for 2 h (ref.[8]) (maghemite 2); commercial recording materials (Hercules, U.S.A.; BASF, Germany) (maghemite 3).

Magnetite (Fe_3O_4). Prepared by oxidation of a $FeSO_4$ solution in a neutral medium with potassium nitrate[8].

Goethite (α-FeOOH). Product of transformation of ferrihydrite in alkaline medium, crystallization at 70 °C for 70 h (goethite 1); commercial SCP 21 material (Société Chimique de Provence, France) (goethite 2); products of basic transformation of ferrihydrite[21] at 4–60 °C and goethite pigments obtained by oxidation of $FeSO_4$ solutions at 40–80 °C and pH 3–4 in the presence of crystallization nuclei (goethite 3).

Lepidocrocite (γ-FeOOH). Lepidocrocites were obtained by oxidation of $FeSO_4$ solution with air[22]. X-Ray diffraction and Moessbauer measurements gave evidence that the samples contained no more than a few percent ferrihydrite and/or goethite.

Ba-Hexaferrite ($BaFe_{12}O_{19}$). Samples were obtained by the citrate method or by hydrolysis of a mixture of metal alkoxides and heating the precipitate at 600 to 900 °C. In one sample, 1/12 Fe was substituted by an equimolar mixture of Co + Ti. The presence of a single ferromagnetic phase was confirmed by magnetic moment measurements. X-Ray measurements revealed no more than a few percent hematite.

Ferrihydrite. Sample obtained by the conventional basic hydrolysis of $Fe(NO_3)_3$, ref.[8] (ferrihydrite 1); samples obtained by boiling iron(III) sulfate solutions with urea (ferrihydrite 2). All ferrihydrite samples were nearly amorphous in X-rays (2-line type[8]). IR spectroscopy revealed a few percent nitrate, sulfate and/or carbonate.

Identity and phase purity of the samples were checked by powder X-ray diffraction, IR, and Moessbauer measurements[10,17]. The particle shape was assessed based on TEM photographs. Specific surface area was determined by the method of adsorption and desorption of a nitrogen–hydrogen mixture using samples pre-dried at 125 °C (for ferrihydrites) or 150 °C (for the remaining substances) for 30 min.

Chronoamperometric Curve Processing

The $I(t)$ dependence was integrated by the trapezoid method to obtain the function $Q(t)$ and the starting value Q_0. Values so obtained were processed by applying Eq. (*2*), which can be easily transformed into a linear form by logarithmization.

Computerized Modelling of the Dissolution Process

In order to obtain the theoretical value of parameter γ, the dissolution process at a constant potential was modelled so that a set of 20 fractions of spherical particles possessing a normal or lognormal distribution of their diameters was created by the SOLO code, and the reaction process was modelled using the SUPERCALC spreadsheet based on the assumption of a linear rate of diminishing of their diameter[23]; the dependence of $S(t)$ on $V(t)$ was processed by applying the equation

$$\frac{S}{V_0} = K\left(\frac{V}{V_0}\right)^{\gamma} , \qquad (5)$$

where K is a constant. The γ values obtained are given in Table I.

RESULTS AND DISCUSSION

Testing the Applicability of the Kinetic Equations

The applicability of the kinetic equation (*2*) to the electrochemical reductive dissolution of iron(III) hydroxy-oxides has been verified[17]. If the dissolution of a sample is conducted in different supporting electrolytes and at different working electrode potentials, then a set of k and γ values is obtained from Eq. (*2*). If parameter γ characterizes the reactive homogeneity (for a single-phase set of particles mirrors the width of their size distribution), its value should be independent of the conditions of measurement. In order to test this, Eq. (*2*) was linearized by logarithmization and rearranged to the form (*6*):

$$\ln\left(\frac{I}{kQ_0}\right) = \gamma \ln\left(\frac{Q}{Q_0}\right) \qquad (6)$$

in which experimental data are inserted for k and Q_0. The normalized values of the variables in Eq. (*6*) give a straight line whose slope is γ, characterizing the set of reacting particles independently of the measuring conditions, as demonstrated by the

TABLE I
Geometrical parameter γ in Eq. (*2*); standard deviations are given in parentheses

Sample	γ
Model of particle sets:[a]	
monodisperse spheres	2/3
spheres with a normal distribution diameters	0.7–0.8
spheres with a lognormal distribution of diameters	>0.8
Published data for real samples:	
dissolution of gypsum[b]	1.16
reductive dissolution of ferrihydrite[c]	1.1
Data for real samples found in this work:[d]	
hematite 1 (4)	1.18(0.15)
hematite 4 (3)	0.93(0.10)
Ba-hexaferrite (3)	1.48(0.18)
goethite 1 (6)	1.27(0.15)
maghemite 1 (2)	0.92(0.10)

[a] Data obtained by computerized modelling of the dissolution process; [b] ref.[16]; [c] ref.[6]; [d] figures in parentheses give the numbers of systems used during chronoamperometric measurements at different working electrode potentials and/or in different supporting electrolytes, one of which was always the hydrogen oxalate buffer.

example shown for hematite 1 in Fig. 1. Table I gives an overview of the average γ values of the other substances examined, in comparison with some published and model data. The differences in the average γ values are significant and their magnitude will be discussed later.

While the chronoamperometric measurements aimed at obtaining the γ values met the requirement of Eq. (*3*), in the DP voltammetric measurement the overall reduction rate in the peak range was determined by the rate of diffusion even at a scan rate of 1 mV s^{-1}, as indicated by the fact that the position of the peak was more negative than the limit of applicability of Eq. (*2*) with γ value constant while retaining applicability of Eq. (*3*). Moreover, DC voltammetry indicates that the dissolution is incomplete (waves similar to those for a diffusion-controlled electrode reaction of soluble ions appear), so that the peak reflects the reaction process in dependence on the mass transport rate near the electrode surface rather than on the consumed amount of sample. To achieve a complete dissolution of the sample during the voltammetric measurement, 1 M HCl must be used and a scan rate in the order of 10^{-1} mV s^{-1} must be applied[24].

Equation (*4*) for the DC peak potential was derived allowing for both the finite diffusion rate and the reacting particles diminishing during the reaction. Assuming that the position of the DP voltammetric peak is shifted from the DC voltammetric peak by a constant which is determined by the charge transfer coefficient and the pulse parameters, we tested the applicability of an equation similar to Eq. (*4*) for the DP mode at a scan rate of 1 mV s^{-1}. The dependence of the DP voltammetric peak potential on the rate constant k_0 obtained for the reduction of α-FeOOH, α-Fe_2O_3, and Ba-hexaferrite in 0.1 M HCl is shown in Fig. 2. The slope of the plot of the DP voltammetric peak potential, $E_{P,DP}$, on ln *k* is $RT/0.63F$. The charge transfer coefficient obtained by chronoamperometric measurement on two samples of α-Fe_2O_3 and one sample of Ba-hexafer-

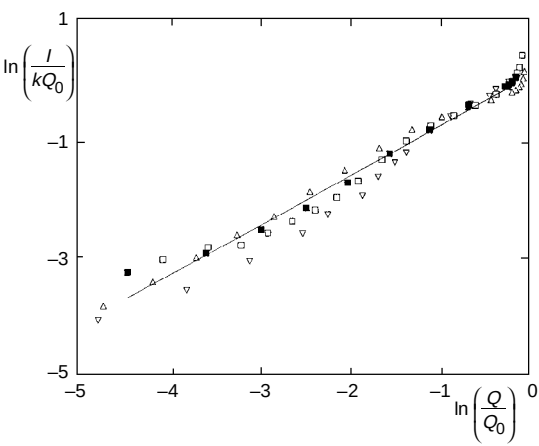

FIG. 1
Chronoamperometric curves of dissolution of hematite 1 normalized by applying Eq. (*7*). Solution composition, potential: ∇ 0.1 M HCl, 0.05 V; Δ MCAA, 0 V; ❒ KHOx, –0.1 V; ■ KHOx, –0.05 V

rite, using Eq. (*3*), has an average value of $\alpha = 0.60$. This group of substances crudely obeys the equation

$$E_{P,DP} = A + \frac{RT}{\alpha nF} \ln k_0 \ , \qquad (7)$$

where constant A incorporates the function of pulse parameters in the DP potential program and, by Eq. (*4*), the function of the average charge transfer coefficient α and the scan rate.

The rate constant k in Eqs (*1*) and (*2*) is dependent on the starting specific surface area of the sample. For the sake of comparability of the rate constants of the individual phases in the solution, the k values were related to a unit surface area[1–5,11]. Therefore,

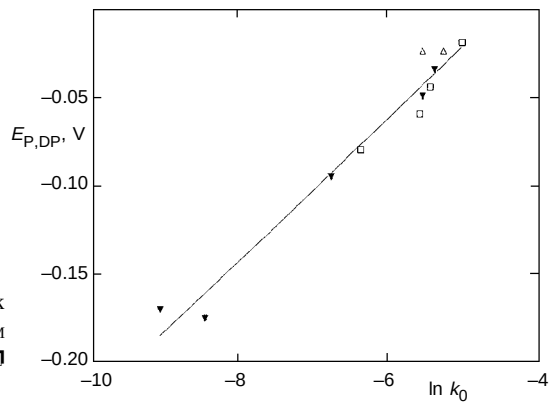

FIG. 2
Dependence of the DP voltammetric peak potential on the rate constant k_0 in 0.1 M HCl. Substance: Δ goethite, ▼ hematite, ❒ Ba-hexaferrite

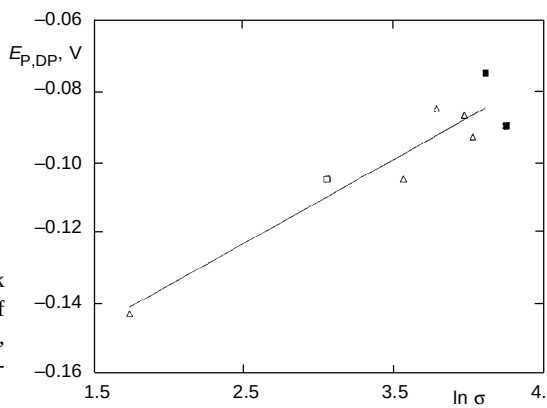

FIG. 3
Dependence of the DP voltammetric peak potential on the specific surface area of sample for the reduction of hematite 1 (∇), hematite 3 (Δ), hematite 5 (❒), and hematite 6 (■) in MCAA solutions

comparison of the DP voltammetric peak potentials with the corresponding specific surface area values σ is of interest. In accordance with Eq. (*7*), the plots of $E_{P,DP}$ vs ln σ are linear (Figs 3 and 4, Table II). The equation in Table II is in the form of

$$E_{P,DP} = B + \frac{RT}{\alpha n F} \ln \sigma \quad . \qquad (8)$$

TABLE II
Dependences of the DP voltammetric peak potentials $E_{P,DP}$ on the logarithm of the specific surface area σ. Supporting electrolyte: MCAB. Either the regression Eq. (*8*) or the average, with the standard deviation in parentheses, is given

Phase (number of samples)	$E_{P,DP}$, V
Ba-Hexaferrite (3) and hematite (8)	$-0.33 + \frac{RT}{0.63F} \ln \sigma$ [a]
Goethite (10)	$-0.32 + \frac{RT}{0.92F} \ln \sigma$ [b]
Maghemite (4) and magnetite (1)	$-0.19 + \frac{RT}{0.83F} \ln \sigma$ [c]
Lepidocrocite (4)	+0.03(0.01)[d]
Ferrihydrite (4)	+0.03(0.01)[e]

Regression coefficient: [a] $r = 0.759$; [b] $r = 0.733$; [c] $r = 0.858$; range of σ: [d] 30–200 $m^2 g^{-1}$; [e] 100–400 $m^2 g^{-1}$.

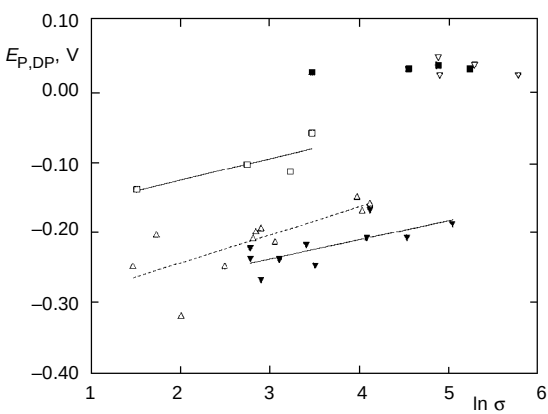

FIG. 4
Dependence of the DP voltammetric peak potential on the specific surface area of sample for the reduction of goethite (▼), hematite and Ba-hexaferrite (Δ), maghemite and magnetite (❒), lepidocrocite (■), and ferrihydrite (▽) in MCAB solutions; statistically significant linear dependences of $E_{P,DP}$ on ln σ are indicated by straight lines

This dependence does not hold for lepidocrocite and ferrihydrite; these are phases exhibiting the highest proton-promoted dissolution rates[5], and so it is conceivable that the mechanism of their electrochemical dissolution is somewhat different and the charge transfer rate is not the only limiting factor in the overall reaction rate.

Effect of Phase Composition on Electrochemical Behaviour

During its electrochemical reduction, each sample is characterized by its specific surface area (Eq. (*8*)), rate constant per a unit surface area (which is typical of the phase in question and is involved in constant *B*), the charge transfer coefficient, and the reactivity distribution, which is mirrored by the factor γ. The last-mentioned parameter, for a phase-uniform sample, is not determined by the particle and solution composition; instead, it is determined by the geometrical properties of the particles solely. The remaining parameters can be affected by the phase composition.

Hematite and Ba-Hexaferrite

The reactivity of a unit surface area of the phases is similar, as their structure is. Both phases have (like goethite) the hexagonal close-packed arrangement of the oxide anions in the crystal lattice[8], which is responsible for their low reactivity during dissolution[3]. The dissolution rate constants in 0.1 M HCl per unit surface area are given in Table III. The appreciable differences between the samples indicate that the degree of perfectness

TABLE III
Rate constants k_0 and their relative values per unit surface area during the reductive dissolution of samples of hematite, Ba-hexaferrite, and goethite in 0.1 M HCl

Sample	k_0, 10^{-3} s^{-1}	$\frac{k_0}{\sigma}$, 10^{-5} g s^{-1} m^{-2}
Goethite 1	5.4	25
Goethite 2	4.1	26
Hematite 1	4.8	86
Hematite 2	1.2	21
Hematite 3	4.1	25
Hematite 4	0.22	1.8
Ba-hexaferrite	4.5	105
	1.8	50
Ba-Co, Ti-hexaferrite	0.15	9.5

of the crystal structure plays a major role; for instance, hydrothermal hematite 1 dissolves fastest, while a simple thermal dehydration (hematite 2) brings about a decrease in this rate to one-quarter. Consistent with this is the dissolution of hematite in dilute acid, where large individual differences in reactivity have been observed for samples of different origin[11]. Due to this, the $E_{P,DP}$ vs ln σ plot for the MCAB solutions possesses a regression coefficient as low as $r = 0.759$ (Table II). The plot is statistically more significant if hematites 1, 3, 5, and 6 only are included ($r = 0.887$); these are samples in whose crystal lattice water can be present because they have been prepared from aqueous solutions or by dehydration of FeOOH and ferrihydrite. The corresponding average charge transfer coefficient obtained based on Eq. (*8*) is $\alpha = 0.93$.

Goethite

The dissolution of goethite is anisotropic, and hence, dependent on the nature of the particles[1,2,10]. The dependence expressed by Eq. (*8*) is only roughly satisfied, because anisotropy is not taken into account by this equation. However, as noted by us earlier[10], the effect of anisotropy on the voltammetric curve shape can be suppressed by using 0.1 M HCl and applying a low scan rate. Data in Table II indicate that the DP voltammetric peak potential is statistically significantly dependent on ln σ whereas the values of constant *B* in Eq. (*8*) do not differ significantly within the hematite and Ba-hexaferrite group, apparently due to a similar structure of the substances. Consistent with this is the lowest rate of their chemical dissolution[3–6].

Oxides Possessing the Spinel Structure

The structures of the two oxides, Fe_3O_4 and γ-Fe_2O_3, approach each other closely owing to the cubic close-packed arrangement of the oxide ions in their lattices[8]. The DP voltammetric peak potentials of magnetite and of maghemite prepared from it differ by a few millivolts only. Dissolution in HCl has been reported to be faster for magnetite than for maghemite[5], which may be due to the presence of Fe^{2+} in the magnetite dissolution products. Although the Fe^{3+}/Fe^{2+} system is irreversible in HCl, the dissolution rate is determined by the redox potential in the surroundings of the particle[7]. During the reductive dissolution, however, this effect does not appear because all iron ions in the surroundings of the particle are present in the divalent oxidation state. The $E_{P,DP}$ vs ln σ plot for this group of substances exhibits the highest regression coefficient.

Particle Shape Homogeneity

As mentioned above, the value of parameter γ (Table I) generally depends on the reactive homogeneity of the particles. The facts reported also document that a phase purity on its own does not guarantee a uniform reactivity of the particles. For α-FeOOH and α-Fe_2O_3, values of $\gamma > 1$ can imply a continuous distribution of unit surface area reactivity of otherwise monodisperse particles. For instance, hydrothermal hematite 1 and goethite 1 exhibit higher γ values (Table I). The high γ value of Ba-hexaferrite, however, seems to be due to the high temperature of preparation (750 °C), at which particle sintering takes place[8], increasing the particle shape and size diversity. Samples of hematite 4 and maghemite 1 can be regarded as highly homogeneous sets as far as their reactivity is concerned, approaching the model of isotropic spheres with a lognormal distribution of their diameters[20].

Phase Transformations

Phase transformations of the particles can bring about changes in their reactivity per unit surface area, associated with the appearance of a new DP voltammetric peak (such as during the conversion of γ-Fe_2O_3 to α-Fe_2O_3), as well as a disturbance of the shape of the crystals (such as during the dehydration of FeOOH), and recrystallization or sintering of the particles. Changes in the dissolution rate constant during the formation of a less reactive phase can be examined voltammetrically and chronoamperometri-

TABLE IV
Electrochemical parameters of lepidocrocite and its transformation products during heating for 30 min; voltammetric measurements in MCAB, chronoamperometric measurements in potassium hydrogen oxalate at $E = -0.1$ V

Temperature °C	Water loss %	$E_{P,DP}$, V	Dissolution reaction parameters		Phase composition
			k, 10^{-3} s^{-1}	γ	
		0.01	12	1.2	lepidocrocite
180	1.7	0.00	18	1.5	"
240	10	–0.01	20	1.3	maghemite
290	10	–0.02	23	1.5	"
345		–0.02	25	1.6	"
390		–0.03	30	2.1	"
440		–0.18	7	2.0	hematite
500		–0.19	5	1.9	"

cally, whereas recrystallization, which gives rise to a change in shape homogeneity and, hence, in the γ value, can be measured chronoamperometrically.

The results of electrochemical measurement of the dissolution characteristics of γ-FeOOH during heating, which is associated with two phase transformations, are given in Table IV. During the first transformation, dehydration gives rise to topotactic γ-Fe_2O_3 with a large specific surface area. The DP voltammetric peak measured in a monochloroacetate buffer is cathodically shifted, the dissolution rate in oxalate buffer doubles, and the γ value increases as well. The reactivity decrease is even more pronounced during the transformation to α-Fe_2O_3; the γ parameter also grows due to the fact that this transformation is not topotactic and hence, is associated with a considerable particle recrystallization.

Due to the similarity of the phases, the dehydration of α-FeOOH to α-Fe_2O_3 is not accompanied by a substantial change in the dissolution rate, only the γ value increases slightly. The DP voltammetric curve displays a goethite peak shape change right before the dehydration and, in particular, a single sharp peak of hematite appearing. DTA and DTG measurements indicate that the dehydration of larger goethite particles proceeds in two steps[25,26]. In accordance with this is the sequence of changes as shown in Fig. 5 for goethite 1. First, the DP voltammetric curve possesses a shape typical for anisotropic dissolution[10]. After heating to 220 °C, the substance loses 3–5% water and a single voltammetric peak appears; its anodic shift suggests a temporary surface area increase due to the formation of dehydration pores. A complete loss of water takes place at temperatures in excess of 240 °C. The DP voltammogram displays a single peak of hematite, which shifts cathodically by mere tens of millivolts at 280–400 °C,

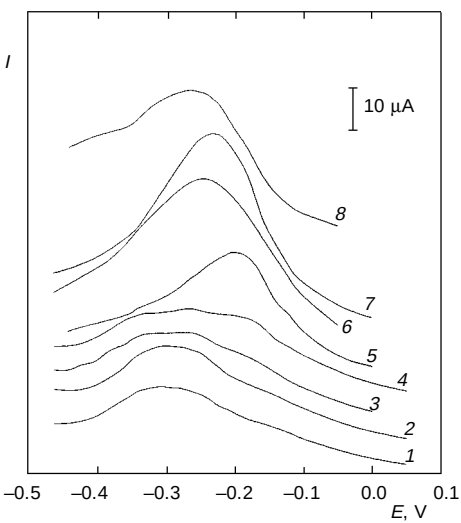

FIG. 5
Changes in the DP voltammetric curve shapes for goethite 1 (curve *1*) heated at 110 (*2*), 180 (*3*), 220 (*4*), 240 (*5*), 280 (*6*), 380 (*7*), and 500 °C (*8*) in MCAB supporting electrolyte; DP pulse: at –12.5 mV in 0.2 s periods, scan rate: 10 mV s^{-1}

presumably due to recrystallization of the dehydration pores. The dehydration of goethite 2 and the goethite pigment Bayer No. 940 follows the same patterns.

CONCLUSIONS

The rate of reductive dissolution of iron(III) hydroxy-oxides in solutions at a given pH and ionic composition[17] is affected: (i) by the phase composition of the particles, which influences their reaction rate as well as the charge transfer coefficient during the reduction; (ii) for α-FeOOH, by the crystal shape, and for α-Fe_2O_3, by the preparation method (degree of perfectness of the crystal structure); and (iii) by the particle size distribution, which can be expressed through parameter γ (Eq. (*2*)).

The DP voltammetric peak potential is determined by the rate constant k_0 at a reference potential and the charge transfer coefficient, which can be obtained by processing the chronoamperometric curves based on Eqs (*2*) and (*3*). Electrochemical reductive dissolution of iron(III) hydroxy-oxides can serve the analysis of the phase composition, assessment of the particle size for a known phase composition, and evaluation of the particle size distribution or phase heterogeneity.

SYMBOLS

AbrSV	abrasive stripping voltammetry[13,14]
DC	direct current mode
DP	differential pulse mode
E	working electrode potential vs SCE, V
$E_{P,DP}$	DP voltammetric peak potential, V
F	Faraday constant
k	pseudo-first order rate constant, s^{-1}
k_0	rate constant at the reference electrode potential, s^{-1}
n	number of exchanged electrons per Fe atom
N	amount of substance reacting in a given time, mol
N_0	total starting amount of reactant, mol
Q, Q_0	charge corresponding to the amount of substance N or N_0, respectively, C
r	regression coefficient
S	total surface area of the set of particles, m^2
v	scan rate, V s^{-1}
V, V_0	total volume of set of particles in time t and at $t = 0$, m^3
α	charge transfer coefficient
γ	dimensionless parameter of reactive homogeneity of the particle set (Eqs (*1*) and (*2*))
σ	specific surface area, $m^2\ g^{-1}$

The author wishes to thank Dr F. Hanousek, Mr J. Bohacek, Mr V. Stengl and Mr. J. Bursik (Institute of Inorganic Chemistry, Academy of Sciences of the Czech Republic) for some of the samples employed in this work.

REFERENCES

1. Cornell R. M., Posner A. M., Quirk J. P.: J. Inorg. Nucl. Chem. *36*, 1937 (1974).
2. Cornell R. M., Posner A. M., Quirk J. P.: J. Inorg. Nucl. Chem. *38*, 563 (1976).
3. Siddhu P. S., Gilkes R. J., Cornell R. M., Posner A. M., Quirk J. P.: Clays Clay Miner. *29*, 269 (1981).
4. Zinder B., Furrer G., Stumm W.: Geochim. Cosmochim. Acta *50*, 1861 (1986).
5. Biber M., Alfonso M. S., Stumm W.: Geochim. Cosmochim. Acta *58*, 1999 (1994).
6. Postma D.: Geochim. Cosmochim. Acta *57*, 5027 (1993).
7. Mancey D. S., Shoesmith D. W., Lipkowski J., McBride A. C., Noel J.: J. Electrochem. Soc. *140*, 637 (1993).
8. Schwertmann U., Cornell R. M.: *Iron Oxides in the Laboratory*. Verlag Chemie, Weinheim 1991.
9. Tessier A., Campbell P. G. C., Bisson M.: Anal. Chem. *51*, 844 (1979).
10. Grygar T., Subrt J., Bohacek J.: Collect. Czech. Chem. Commun. *60*, 950 (1995).
11. Cornell R. M., Giovanoli R.: Clay Miner. *28*, 223 (1993).
12. Barinina Kh. Z., Vydrevich M. B.: J. Electroanal. Chem. *121*, 1 (1981).
13. Scholz F., Nitschke L., Henrion G.: Naturwissenschaften *76*, 71 (1989).
14. Scholz F., Lange B.: Trends Anal. Chem. *11*, 359 (1992).
15. Hickling A., Ives D. J. G.: Electrochim. Acta *20*, 63 (1975).
16. Christoffersen J., Christoffersen M. R.: J. Cryst. Growth *35*, 79 (1976).
17. Grygar T.: Collect. Czech. Chem. Commun. *60*, 1261 (1995).
18. Subrt J., Solcova A., Hanousek F., Petrina A., Zapletal V.: Collect. Czech. Chem. Commun. *47*, 2478 (1984).
19. Subrt J., Hanousek F., Zapletal V., Stepankova H.: J. Mater. Sci. *17*, 215 (1982).
20. Subrt J.: Unpublished results.
21. Schwertmann U.: Clays Clay Miner. *33*, 369 (1985).
22. Solcova A., Subrt J., Hanousek F., Holba P., Zapletal V., Lipka J.: Silikaty *24*, 133 (1980).
23. Compton R. G., Brown C. A.: J. Colloid Interface Sci. *158*, 243 (1993).
24. Mouhandess M. T., Chassagneux F., Vittori O.: J. Electroanal. Chem. *131*, 367 (1982).
25. Derie R., Ghodsi M., Calvo-Roche C.: J. Therm. Anal. *9*, 435 (1976).
26. Schwertmann U.: Thermochim. Acta *78*, 39 (1984).